

Published in final edited form as:

Curr Biol. 2012 April 10; 22(7): 638–644. doi:10.1016/j.cub.2012.02.030.

Checkpoint-independent stabilization of kinetochore-microtubule attachments by Mad2 in human cells

Lilian Kabeche and Duane A. Compton*

Department of Biochemistry, Dartmouth Medical School, Hanover, NH 03755; Norris Cotton Cancer Center, Lebanon, NH 03756, USA

Summary

Faithful chromosome segregation is required for cell and organism viability and relies on both the mitotic checkpoint and the machinery that corrects kinetochore-microtubule (k-MT) attachment errors [1–3]. Most solid tumors have aneuploid karyotypes and many mis-segregate chromosomes at high rates in a phenomenon called chromosomal instability (CIN) [4–6]. Mad2 is essential for mitotic checkpoint function and is frequently overexpressed in human tumors that are CIN [1,7–13]. For unknown reasons, cells overexpressing Mad2 display high rates of lagging chromosomes [14,15]. Here, we explore this phenomenon and show that k-MT attachments are hyperstabilized by Mad2 overexpression and that this undermines the efficiency of correction of k-MT attachment errors. Mad2 affects k-MT attachment stability independently of the mitotic checkpoint because k-MT attachments are unaltered upon Mad1 depletion and Mad2 overexpression hyperstabilizes k-MT attachments in Mad1-deficient cells. Mad2 mediates these effects with Cdc20 by altering the centromeric localization and activity of Aurora B kinase, a known regulator of k-MT attachment stability. These data reveal a new function for Mad2 to stabilize k-MT attachments independent of the checkpoint and explains why Mad2 overexpression increases chromosome mis-segregation to cause chromosomal instability in human tumors.

Results

Many human tumors that are aneuploid and CIN and overexpress the conserved checkpoint protein Mad2 [7–13]. Moreover, mice engineered to overexpress Mad2 develop tumors that are CIN [14,15]. Interestingly, cells derived from mouse models overexpressing Mad2 display elevated frequencies of lagging chromosomes in anaphase [14,15] raising the possibility that Mad2 plays a role as a component of the machinery that regulates k-MT attachment stability to promote the correction of attachment errors needed for faithful chromosome segregation. To determine if Mad2 influences the stability of k-MT attachments during mitosis we measured the dynamics of k-MTs in cells expressing photoactivatable GFP-tubulin (PA-GFP-tubulin). We expressed PA-GFP-tubulin in non-transformed, diploid, chromosomally stable human RPE-1 cells and used fluorescence dissipation after photoactivation of spindle microtubules to determine the stability of k-MT attachments (Figure 1A) [3,16,17]. Fluorescence decay of the activated region fit a double exponential curve ($r^2 > 0.99$) where the rapidly decaying fluorescence corresponds to non-k-

© 2012 Published by Elsevier Inc.

*corresponding author, Department of Biochemistry, 413 Remsen Bldg., Dartmouth Medical School, Hanover, N.H. 03755, Tel: (603) 650-1990, FAX: (603) 650-1128, duane.a.compton@dartmouth.edu.

Publisher's Disclaimer: This is a PDF file of an unedited manuscript that has been accepted for publication. As a service to our customers we are providing this early version of the manuscript. The manuscript will undergo copyediting, typesetting, and review of the resulting proof before it is published in its final citable form. Please note that during the production process errors may be discovered which could affect the content, and all legal disclaimers that apply to the journal pertain.

MTs and the slowly decaying fluorescence corresponds to k-MTs (Figure 1B). Non-k-MTs turn over with a half-life ($t_{1/2}$) of approximately 14.4 ± 0.1 sec in prometaphase and 15.6 ± 0.1 sec in metaphase and there was no detectable change in these rates in any of our experimental conditions. K-MTs are more stable during mitosis and display $t_{1/2}$ of 1.8 ± 0.6 min and 3.8 ± 1.1 min in prometaphase and metaphase, respectively, in untreated RPE-1 cells (Figure 2).

Next, we examined k-MT attachment stability in cells depleted of the conserved checkpoint protein Mad2. Mad2 depletion was confirmed by immunoblot and by reductions in the mitotic index of cells in the presence of the microtubule perturbing drug nocodazole indicating functional loss of checkpoint activity (Figure S1). To prevent premature anaphase onset caused by the absence of a functional mitotic checkpoint in the absence of Mad2, we measured k-MT turnover in Mad2-deficient mitotic cells treated with the proteasome inhibitor MG-132 (5 μ M). Delaying anaphase onset using MG-132 does not significantly change k-MT stability relative to control cells in either prometaphase or metaphase (Figure 2) regardless of the length of time that cells were blocked in metaphase (we tested up to 4 hours). The half-life of k-MT attachments in Mad2-deficient cells was significantly reduced relative to control cells in both prometaphase and metaphase (Figure 2). To eliminate potential off-target effects of the siRNA, we depleted Mad2 using an siRNA sequence derived from the 3' UTR and rescued the loss of Mad2 by exogenous expression of mCherry-Mad2 (Figure S1). Mad2 depletion using this siRNA sequence was confirmed by immunoblot and loss of checkpoint function in the presence of nocodazole (Figure S1). The half-life of k-MT attachments in cells depleted of Mad2 using this siRNA sequence was reduced compared to control cells to an extent that was equivalent to cells depleted with the other siRNA sequence (Figure S1). Overexpression of mCherry-Mad2 in these Mad2-deficient cells restored both the checkpoint function and k-MT stability indicating a specific requirement for Mad2 to regulate k-MT attachment stability.

To determine if the change in k-MT attachment stability was accounted for by loss of checkpoint activity we measured k-MT turnover in cells depleted of another conserved checkpoint protein Mad1. Mad1 depletion was confirmed by immunoblot and by reductions in the mitotic index of cells in the presence of the microtubule perturbing drug nocodazole indicating functional loss of checkpoint activity (Figure S1). In contrast to Mad2-deficient cells, there was no significant change in the half-life of k-MT attachments in Mad1-deficient cells in either prometaphase or metaphase relative to control cells (Figure 2). This demonstrates that Mad2 stabilizes k-MT attachments during both prometaphase and metaphase independently of Mad1.

We next tested the contribution of other proteins involved in the metaphase-anaphase transition to k-MT attachment stability by depleting cells of either BubR1 or Cdc20. We confirmed efficient depletion of BubR1 by immunoblot and by reductions in the mitotic index of cells in the presence of the microtubule perturbing drug nocodazole indicating functional loss of checkpoint activity (Figure S1). BubR1 has a known role in stabilizing k-MT attachments [18–20]. Accordingly, we observed significant reductions in the half-life of k-MT attachments in BubR1-deficient cells in both prometaphase and metaphase (Figure 2). Kinetochore-MTs in cells simultaneously depleted of both Mad2 and BubR1 are significantly less stable than cells depleted of BubR1 alone in both prometaphase and metaphase (Student's *t*-test; $p=0.04$ in prometaphase, $p=0.02$ in metaphase) demonstrating that BubR1 and Mad2 contribute to the stabilization of k-MTs through independent pathways (Figure 2). The depletion of Cdc20 was confirmed by immunoblot and by increases in mitotic index indicating a failure to efficiently activate the APC/C to induce anaphase onset (Figure S1). The half-life of k-MT attachments in Cdc20-deficient mitotic cells was significantly reduced relative to control cells in both prometaphase and metaphase (Figure

2), yet indistinguishable from cells lacking Mad2 alone. The half-life of k-MT attachments in cells depleted of both Cdc20 and Mad2 in both prometaphase and metaphase was not significantly different from cells depleted of either Cdc20 or Mad2 alone (Figures 2 and S1) demonstrating that Mad2 and Cdc20 act in the same pathway to stabilize k-MT attachments during mitosis.

To test if excess levels of Mad2 hyperstabilize k-MT attachments we overexpressed Mad2 and measured k-MT attachment stability. Transient expression of mCherry-Mad2 was detected by immunoblot and fluorescence imaging in most cells (Figure S2). As expected, it localized to kinetochores in prometaphase cells (Figure S2). The expression level of mCherry-Mad2 under these conditions was estimated to be approximately 5- to 10-fold higher than endogenous protein levels. There was little change in the mitotic index of cells overexpressing mCherry-Mad2 consistent with only a 2-fold increase in time spent between prometaphase and anaphase measured previously in mouse cells overexpressing Mad2 [14]. The attachment stability of k-MTs in cells overexpressing mCherry-Mad2 was significantly increased compared to control cells in both prometaphase and metaphase (Figures 1A and 2). We next tested the effects of overexpression of mutant versions of Mad2 including mCherry-Mad2 Δ C, -Mad2V193N, and -Mad2R133A [21–22]. The level of overexpression of each protein was equivalent to mCherry-Mad2 (Figure S2). Neither Mad2 Δ C nor Mad2V193N altered k-MT attachment stability indicating that Mad2 must be capable of converting to a closed conformation to influence k-MT attachments (Figure 2). In contrast, Mad2R133A stabilized k-MT attachments indicating that Mad2 does not need to dimerize to influence k-MT attachments (Figure 2). Finally, to test if k-MT stabilization by excess Mad2 requires a functional mitotic checkpoint we overexpressed mCherry-Mad2 in Mad1-deficient cells. Immunoblot analyses verify the overexpression of mCherry-Mad2 and the efficient depletion of Mad1 (Figure S1). Overexpression of mCherry-Mad2 increased the half-life of k-MT attachments to similar extents in mitotic cells with or without Mad1 (Figure 2). Thus, overexpression of Mad2 hyperstabilizes k-MT attachments through a mechanism that is independent of the Mad1-dependent mitotic checkpoint.

The consequence of increasing k-MT attachment stability is reduced correction of k-MT attachment errors such as merotelic that manifest as lagging chromosomes in anaphase [3,5,6,23]. Overexpression of mCherry-Mad2 significantly increases the frequency of anaphase cells with lagging chromosomes in human RPE-1 cells (Figure 3A and B). Overexpression of mCherry-Mad2 Δ C does not alter the frequency of lagging chromosomes in anaphase (Figure 3B) consistent with the lack of change in k-MT attachment stability when this mutant version of Mad2 is overexpressed. To verify that the hyperstabilization of k-MT attachments induced by Mad2 overexpression is the root cause of lagging chromosomes in anaphase we overexpressed the kinesin-13 protein MCAK which has been demonstrated to destabilize k-MT attachments [3]. The frequency of lagging chromosomes in anaphase in cells overexpressing both Mad2 and MCAK was much lower than cells expressing Mad2 alone and not significantly different from untreated cells (Figure 3A and B). Similar results were obtained using U2OS cells that are aneuploid and CIN and have an inherently high basal rate of lagging chromosomes in anaphase owing to CIN (Figure S3). Thus, Mad2 overexpression undermines the correction of k-MT attachment errors by hyperstabilizing k-MT attachments. This elevates chromosome mis-segregation rates through the most common mechanism known to cause CIN in human tumor cells.

To explore the mechanism through which Mad2 stabilizes k-MT attachments we examined the localization of Aurora B and BubR1, two known regulators of k-MT attachment stability [18–20,23–25]. The quantity of Aurora B localized to centromeres was significantly increased by Mad2 depletion and significantly decreased by Mad2 overexpression in both prometaphase and metaphase (Figures 4A and B). The functional activity of Aurora B was

similarly influenced by Mad2 levels as judged by alterations in the quantities of Aurora B substrates CenpA (Figure 4C) [26] and histone H3 (data not shown). Mad2 levels also affect the quantity and activity of Aurora B kinase at centromeres in nocodazole-treated mitotic cells (Figure S4) indicating that these events are independent of microtubule attachment at kinetochores. Moreover, sister kinetochore spacing was unchanged in both prometaphase and metaphase by either overexpression or depletion of Mad2 indicating that Aurora B activity is regulated independently of the spatial positioning of sister kinetochores under these conditions. In contrast, changing Mad2 levels did not significantly affect the quantity of BubR1 localized at kinetochores indicating a specific response of Aurora B to Mad2 levels (Figure 4D). It has been shown that k-MT attachment stability is acutely sensitive to Aurora B function [23,27], and these data demonstrate that Mad2 attenuates the degree to which Aurora B kinase destabilizes k-MT attachment stability.

Discussion

Combined, these data demonstrate that Mad2 stabilizes k-MT attachments in mammalian cells. This new function of Mad2 is independent of the spindle assembly checkpoint because it acts in both prometaphase and metaphase and does not rely on Mad1. Mad2 protein levels in mitotic cells exceed those of Mad1 by approximately 10-fold [28]. Thus, soluble pools of Mad2 are available for checkpoint-independent functions if Mad1 limits the quantity of Mad2 entering the checkpoint signaling pathway. These data support a model whereby Mad2 stabilizes k-MT attachments independently of targeting to kinetochores. A soluble pool of Mad2 alters the quantity and activity of Aurora B kinase at centromeres to influence k-MT attachment stability (Figure 4E). The conversion of Mad2 from the open to closed conformation is necessary for this new function indicating that a fraction of Mad2 undergoes that conformational switch in the cytosol. The conformational change in this cytosolic fraction of Mad2 may be induced through interactions with Cdc20 as suggested previously [21,22,29] without targeting to the kinetochore. Evidence supporting this view comes from our data showing that Mad2 and Cdc20 appear to be acting in the same pathway to influence k-MT stability and other work showing that Mad2-Cdc20 complexes exist independently of the checkpoint-generated mitotic-checkpoint complex [30,31], that Mad2 and Cdc20 can form a complex in the absence of functional kinetochores [30,32], and that the Mad2-Cdc20 complex persists in metaphase cells that lack the mitotic-checkpoint complex [33]. This new function for Mad2 may be related to how it promotes the reorientation of misaligned chromosomes during meiosis 1 in budding yeast [34].

In addition to Mad2, several other components of the spindle assembly checkpoint have been implicated in regulating k-MT attachments based on MT density in spindles [19] or their requirement for efficient chromosome congression during mitosis [35–39]. Most of these checkpoint proteins appear to exert their effects by influencing Aurora B kinase activity. At present, the molecular details for how any of these checkpoint proteins influence Aurora B activity remains unknown, but our evidence shows that there are at least two separate pathways. Since neither Mad2 nor CDC20 co-localize with Aurora B at centromeres, there must be molecular intermediates in this pathway (Figure 4E), and one candidate is the centromeric protein Sgo2 that has recently been shown to bind Mad2 [40]. Finally, we show that overexpression of Mad2 hyperstabilizes k-MT attachments (Figure 4E) which impairs the correction of k-MT attachment errors such as merotelically. This is consistent with data showing that many tumor cells have a functional checkpoint [41] and that the persistence of k-MT attachment errors is the root cause of CIN in most human tumor cells [2,6]. Thus, our data provide a direct explanation for the prevalence of CIN in tumor cells that overexpress Mad2 such as those caused by loss of RB function [42,43].

Experimental Procedures

Cell transfection

Plasmid transfections were done with FuGENE 6 (Roche Diagnostics), siRNA transfections were conducted using Oligofectamine (Invitrogen) and siRNA/plasmid co-transfections were done with X-tremeGene siRNA (Roche Diagnostics). Cells were analyzed 48 hours after transfection by live cell imaging, immunofluorescence, or preparation for immunoblots. RNA duplexes against Mad1 (5'-CCAAAGUGCUGCACAUGAG), BubR1 (5'-GUCUCACAGAUUGCUGCCU), Cdc20 (5'-CCUGCCGUUACAUCCUUC), Mad2 (5'-GCGUGGCAUAUAUCCAUCU) and Mad2 3'UTR (5'-CAGTATAGGTAGGGAGATA) were purchased from Applied Biosystems.

Antibodies

Antibodies used for in this study were: Mad2 (Bethyl Laboratories), Aurora B (Novus Biologicals), BubR1 (Abcam), pCenpA (Cell Signaling), human CREST serum, actin (Seven Hills Bioreagents), and CDC20 (Bethyl Laboratories). Secondary antibodies were conjugated to fluorescein isothiocyanate (FITC) and Texas Red (Jackson ImmunoResearch), Cy5 (Invitrogen), and HRP (Jackson ImmunoResearch). Immunoblots were detected using Lumiglow (KPL) and BioRad Chemidoc XRL+.

Photoactivation

Images were acquired using Quorum WaveFX-X1 spinning disk confocal system (Quorum Technologies Inc., Guelph, Canada) equipped with Mosaic digital mirror for photoactivation (Andor Technology, South Windsor, Connecticut) and Hamamatsu ImageEM camera (Bridgewater, New Jersey). Prometaphase and metaphase cells with bipolar spindles were identified using differential interference contrast (DIC) microscopy. Microtubules were locally activated in one half spindle. Fluorescence images were captured every 15s for 6min with a 100× 1.4 NA oil-immersion objective. DIC microscopy was then used to verify that bipolar spindle was maintained throughout image acquisition and that cells did not enter anaphase. To quantify fluorescence dissipation after photoactivation, pixel intensities were measured within a 1µm rectangular area surrounding the region of highest fluorescence intensity and background subtracted using an equal area from the non-activated half spindle. The values were corrected for photobleaching by determining the percentage of fluorescence loss during 6mins of image acquisition after photoactivation in the presence of 10µM taxol. Fluorescence values for the first 4 mins were normalized to the first time-point after photoactivation for each cell and the average intensity at each time point was fit to a double exponential curve $A1 \times \exp(-k1t) + A2 \times \exp(-k2t)$ using MatLab (Mathworks) where A1 represents the less stable non kinetochore microtubule population and A2 the more stable kinetochore-microtubule population with decay rates of k1 and k2, respectively. The turnover half-life for each process was calculated as $\ln 2/k$ for each population of microtubules.

Immunofluorescence Microscopy

Cells were fixed with ice cold methanol for 15 minutes, washed with Tris-buffered saline with 5% bovine serum albumin (TBS-BSA) with 0.5% Triton X-100 for 5 minutes, and TBS-BSA for 5 minutes. Antibodies were diluted in TBS-BSA + 0.1% Triton X-100 and coverslips incubated for 1hour at room temperature. After which, cell were washed with TBS-BSA for 5 minutes with shaking. Secondary antibodies were diluted in TBS-BSA + 0.1% Triton X-100 and coverslips incubated for 1 hour at room temperature. For pCenpA, all wash buffers were supplemented with 80nM okadaic Acid and 40nM microcystin. Images were acquired with Orca-ER Hamamatsu cooled CCD camera mounted on an

Eclipse TE 2000-E Nikon microscope. 0.2 μ m optical sections in the z-axis were collected with a plan Apo 60X 1.4 NA oil immersion objective. Iterative restoration was performed using Phylum Live software (Improvision). Anaphase chromatids were counted as lagging if they contained centromere staining (using CREST antibody) in the spindle midzone separated from centromeres at the poles.

For quantitative assessments, cells were incubated for 4 h with MG132 (5 μ M), or Nocodazole (100ng/mL) then fixed and stained for AuroraB/pCenA/BubR1, CREST and DNA. Pixel intensities for CREST and AuroraB/pCenA/BubR1 staining were measured in approximately 15 regions over the entire cell. Background fluorescence was subtracted and the ratio of intensities were calculated and averaged over multiple kinetochores from multiple mitotic cells (n = 10 cells).

Highlights

1. The conserved checkpoint protein Mad2 stabilizes kinetochore-microtubule attachments during mitosis
2. This new functional role for Mad2 is independent of the checkpoint
3. Overexpression of Mad2 hyperstabilizes kinetochore-microtubule attachments which undermines the correction of attachment errors
4. This explains why tumor cells that overexpress Mad2 display chromosomal instability

Supplementary Material

Refer to Web version on PubMed Central for supplementary material.

Acknowledgments

This work was supported by National Institutes of Health grants GM51542 (D.A.C) and GM008704 (L.K.).

Abbreviations

CIN	chromosomal instability
k-MT	kinetochore-microtubule

References

1. Musacchio A, Salmon ED. The spindle-assembly checkpoint in space and time. *Nat. Rev. Mol. Cell Biol.* 2007; 8:379–393. [PubMed: 17426725]
2. Cimini D, Howell B, Maddox P, Khodjakov A, Degraffi F, Salmon ED. Merotelic kinetochore orientation is a major mechanism of aneuploidy in mitotic mammalian tissue cells. *J Cell Biol.* 2001; 153:517–527. [PubMed: 11331303]
3. Bakhom SF, Thompson SL, Manning AL, Compton DA. Genome stability is ensured by temporal control of kinetochore-microtubule dynamics. *Nat. Cell. Biol.* 2009; 11:27–35. [PubMed: 19060894]
4. Lengauer C, Kinzler KW, Vogelstein B. Genetic instabilities in human cancers. *Nature.* 1998; 396:643–649. [PubMed: 9872311]
5. Thompson SL, Compton DA. Examining the link between chromosomal instability and aneuploidy in human cells. *J. Cell. Biol.* 2008; 180:665–672. [PubMed: 18283116]

6. Thompson SL, Bakhoun SF, Compton DA. Mechanisms of chromosomal instability. *Curr. Biol.* 2010; 20:R285–R295. [PubMed: 20334839]
7. Alizadeh AA, Eisen MB, Davis RE, Ma C, Lossos IS, Rosenwald A, Boldrick JC, Sabet H, Tran T, Yu X, et al. Distinct types of diffuse large B-cell lymphoma identified by gene expression profiling. *Nature.* 2000; 403:503–511. [PubMed: 10676951]
8. Chen X, Cheung ST, So S, Fan ST, Barry C, Higgings J, Lai KM, Ji J, Dudoit S, Ng IO, et al. Gene expression patterns in human liver cancers. *Mol. Biol. Cell.* 2002; 13:1929–1939. [PubMed: 12058060]
9. Garber ME, Troyanskaya OG, Schluens K, Petersen S, Thaessler Z, Pacyna-Gengelbach M, van de Rijn M, Rosen GD, Perou CM, Whyte RI, et al. Diversity of gene expression in adenocarcinoma of the lung. *Proc. Natl. Acad. Sci. USA.* 2001; 98:13784–13789. [PubMed: 11707590]
10. Hisaoka M, Matsuyama A, Hashimoto H. Aberrant Mad2 expression in soft-tissue sarcoma. *Pathol. Int.* 2008; 58:329–333. [PubMed: 18477210]
11. Kato T, Daigo Y, Aragaki M, Ishikawa K, Sato M, Kondo S, Kaji M. Overexpression of MAD2 predicts clinical outcome in primary lung cancer patients. *Lung Cancer.* 2011
12. Li GQ, Li H, Zhang HF. Mad2 and p53 expression profiles in colorectal cancer and its clinical significance. *World J. Gastroenterol.* 2003; 9:1972–1975. [PubMed: 12970887]
13. Tanaka K, Nishioka J, Kato K, Nakamura A, Mouri T, Miki C, Kusunoki M, Nobori T. Mitotic checkpoint protein hsMAD2 as a marker predicting liver metastasis of human gastric cancers. *Jpn. J. Cancer Res.* 2001; 92:952–958. [PubMed: 11572763]
14. Sotillo R, Hernando E, Diaz-Rodriguez E, Teruya-Feldstein J, Cordon-Cardo C, Lowe S, Benezra R. Mad2 Overexpression promotes aneuploidy and tumorigenesis in mice. *Cancer Cell.* 2007; 11:9–23. [PubMed: 17189715]
15. Sotillo R, Schvartzman J, Socci N, Benezra R. Mad2-induced chromosome instability leads to lung tumour relapse after oncogene withdrawal. *Nature.* 2010; 464:436–440. [PubMed: 20173739]
16. Zhai Y, Kronebusch PJ, Borisy GG. Kinetochore microtubule dynamics and the metaphase-anaphase transition. *J. Cell Biol.* 1995; 131:721–734. [PubMed: 7593192]
17. Bakhoun SF, Genovese G, Compton DA. Deviant kinetochore microtubule dynamics underlie chromosomal instability. *Curr. Biol.* 2009; 22:1937–1942. 2009. [PubMed: 19879145]
18. Elowe S, Hummer S, Uldschmid A, Li X, Nigg EA. Tension-sensitive Plk1 phosphorylation on BubR1 regulates the stability of kinetochore microtubule interactions. *Genes De.* 2007; 21:2205–2219.
19. Lampson MA, Kapoor TM. The human mitotic checkpoint protein BubR1 regulates chromosome-spindle attachments. *Nat. Cell Biol.* 2004; 7:93–98. [PubMed: 15592459]
20. Rahmani Z, Gagou ME, Lefebvre C, Emre D, Karess RE. Separating the spindle checkpoint, and timer functions of BubR1. *J. Cell Biol.* 2009; 187:597–605. [PubMed: 19951912]
21. Luo X, Fang G, Coldiron M, Lin Y, Yu H, Kirshner M, Wagner G. Structure of the Mad2 spindle assembly checkpoint protein and its interaction with Cdc20. *Nat. Struct. Biol.* 2000; 7:224–229. [PubMed: 10700282]
22. Mapelli M, Massimiliano L, Santaguida S, Musacchio A. The Mad2 conformational dimer: structure and implications for the spindle assembly checkpoint. *Cell.* 2007; 131:730–743. [PubMed: 18022367]
23. Cimini D, Wan XH, Hirel CB, Salmon ED. Aurora kinase promotes turnover of kinetochore microtubules to reduce chromosome segregation errors. *Curr. Biol.* 2006; 16:1711–1718. [PubMed: 16950108]
24. Elowe S, Dulla K, Uldschmid A, Li X, Dou Z, Nigg EA. Uncoupling of the spindle-checkpoint and chromosome-congression functions of BubR1. *J. Cell. Sci.* 2009; 123:84–94. [PubMed: 20016069]
25. Hauf S, Cole RW, LaTerra S, Zimmer C, Schnapp G, Walter R, Heckel A, van Meel J, Rieder CL, Peters JM. The small molecule Hesperadin reveals a role for Aurora B in correcting kinetochore-microtubule attachment and in maintaining the spindle assembly checkpoint. *J. Cell Biol.* 2003; 161:281–294. [PubMed: 12707311]
26. Zeitlin S, Shelby R, Sullivan K. CENP-A is phosphorylated by Aurora B kinase and plays an unexpected role in completion of cytokinesis. *J. Cell Biol.* 2001; 155:1147–1157. [PubMed: 11756469]

27. Liu D, Vader G, Vromans MJ, Lampson MA, Lens SM. Sensing chromosome bi-orientation by spatial separation of aurora B kinase from kinetochore substrates. *Science*. 2009; 323:1350–1353. [PubMed: 19150808]
28. Shah JV, Botvinick E, Bonday Z, Furnari F, Berns M, Cleveland DW. Dynamics of centromere and kinetochore proteins; implications for checkpoint signaling and silencing. *Curr. Biol.* 2004; 14:942–952. [PubMed: 15182667]
29. Luo X, Zhanyun T, Rizo J, Yu H. The Mad2 spindle checkpoint protein undergoes similar major conformational changes upon binding to either Mad1 or Cdc20. *Mol. Cell.* 2002; 9:59–71. [PubMed: 11804586]
30. Poodar A, Stukenberg PT, Burke DJ. Two complexes of the spindle checkpoint proteins containing Cdc20 and Mad2 assemble during mitosis independently of the kinetochore in *Saccharomyces cerevisiae*. *Eukaryot. Cell.* 2005; 4:867–878. [PubMed: 15879521]
31. Sudakin V, Chan GKT, Yen T. Checkpoint inhibition of the PAC/C in HeLa cells is mediated by a complex of BUBR1, BUB3, CDC20, and MAD2. *J. Cell Biol.* 2001; 154:925–936. [PubMed: 11535616]
32. Frascini R, Beretta A, Sironi L, Mussacchio A, Lucchini G, Piatti S. Bub3 interaction with Mad2, Mad3, and Cdc20 is mediated by WD40 repeats and does not require intact kinetochores. *The EMBO J.* 2001; 20:6648–6659.
33. Ma HT, Poon RYC. Orderly inactivation of the key checkpoint protein mitotic arrest deficient 2 (Mad2) during mitotic progression. *J. Biol. Chem.* 2010; 286:13052–13059. [PubMed: 21335556]
34. Shonn M, Murray A, Murray A. Spindle Checkpoint Component Mad2 Contributes to Bi-orientation of Homologous Chromosomes. *Curr Biol.* 2003; 13:1979–1984. [PubMed: 14614824]
35. Ditchfield C, Johnson VL, Tighe A, Ellston R, Haworth C, Johnson T, Mortlock A, Keen N, Taylor SS. Aurora B couples chromosome alignment with anaphase by targeting BubR1, Mad2, and Cenp-E to kinetochores. *J Cell Biol.* 2003; 161:267–280. [PubMed: 12719470]
36. Draviam VM, Xie S, Sorger PK. Chromosome segregation and genomic stability. *Curr Opin Genet Dev.* 2004; 14:120–125. [PubMed: 15196457]
37. Jelluma N, Brenkman AB, van der Broek NJF, Cruigesen CWF, van Osch MHJ, Lens SMA, Medema RH, Kops GJPL. Mps1 phosphorylates Borealin to control Aurora B activity and chromosome alignment. *Cell.* 2008; 132:233–246. [PubMed: 18243099]
38. Logarinho E, Resende T, Torres C, Bousbaa H. The human spindle assembly checkpoint protein Bub3 is required for the establishment of efficient kinetochore-microtubule attachments. *Mol. Biol. Cell.* 2008; 19:1798–1813. [PubMed: 18199686]
39. Meraldi P, Sorger PK. A dual role for Bub1 in the spindle checkpoint and chromosome congression. *The EMBO J.* 2005; 24:1621–1633.
40. Orth M, Mayer B, Rehm K, Ulli R, Heidmann D, Holak TA, Stemmann O. Shugoshin is a Mad1/Cdc20-like interactor of Mad2. *The EMBO J.* 2011; 30:2868–2880.
41. Tighe A, Johnson VL, Albertella M, Taylor SS. Aneuploid colon cancer cells have a robust spindle checkpoint. *EMBO Rep.* 2001; 2:609–614. [PubMed: 11454737]
42. Schwartzman JM, Dujif PH, Sotillo R, Coker C, Benezra R. Mad2 is a critical mediator of the chromosome instability observed up Rb and p53 pathway inhibition. *Cancer Cell.* 2011; 19:701–714. [PubMed: 21665145]
43. Hernando E, Nahle Z, Juan G, Diaz-Rodriguez E, Alaminos M, Hemann M, Michel L, Mittal V, Gerald W, Benezra R, et al. Rb inactivation promotes genomic instability by uncoupling cell cycle progression from mitotic control. *Nature.* 2004; 430:797–802. [PubMed: 15306814]

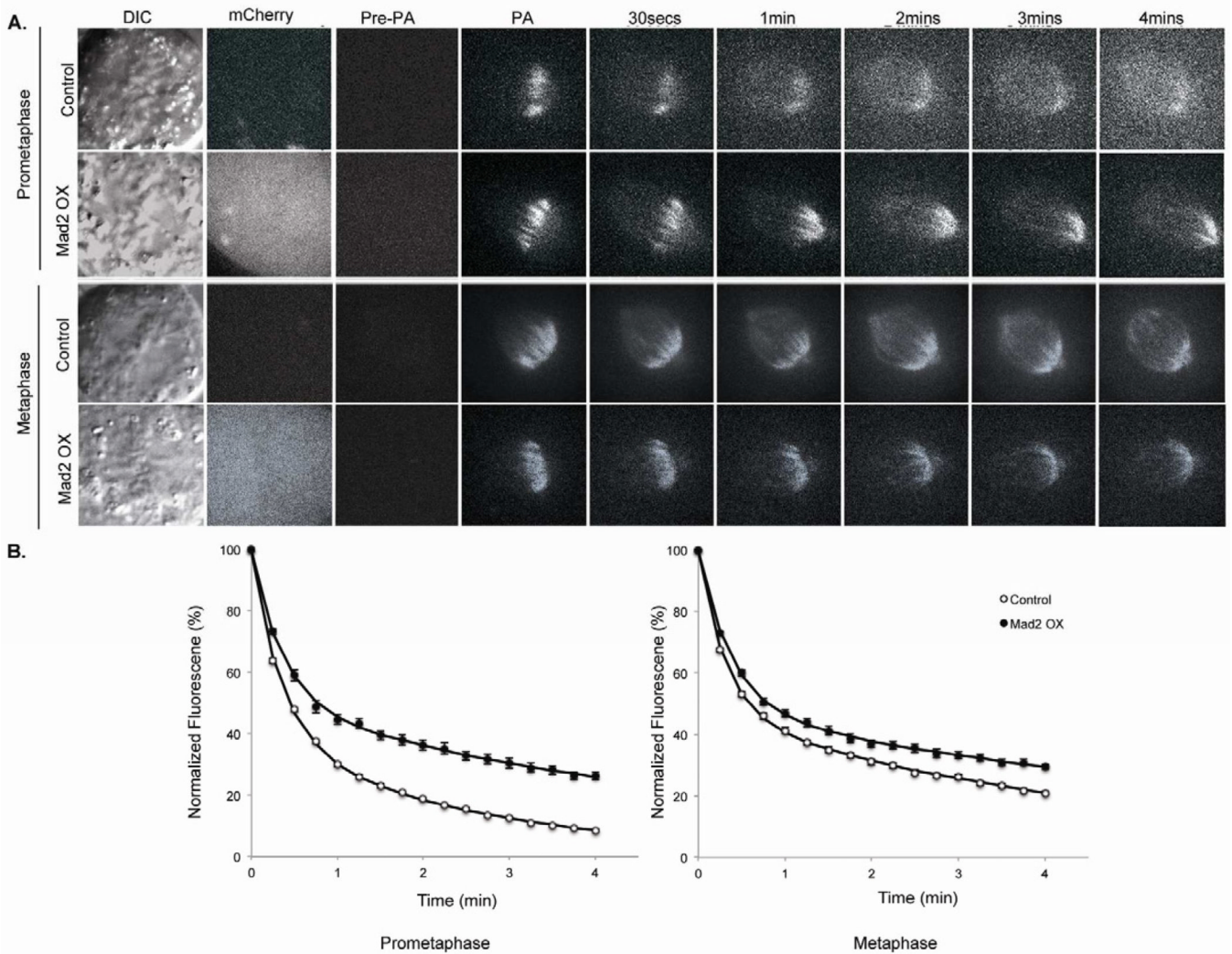


Figure 1.

Measurement of kinetochore-microtubule dynamics in cells overexpressing Mad2. (A) DIC and time-lapse fluorescent images of prometaphase and metaphase spindles in untreated (control) and Mad2 overexpression (Mad2OX) in PA-GFP tubulin expressing RPE1 cells before (Pre-PA) and at indicated times after photoactivation. Mad2 overexpression is visualized by mCherry fluorescence. (B) Normalized fluorescence intensity over time after photoactivation of spindles in untreated (white circles) and Mad2OX (filled circles) in prometaphase and metaphase cells. Data represents mean \pm s.e.m., $n \geq 10$ cells.

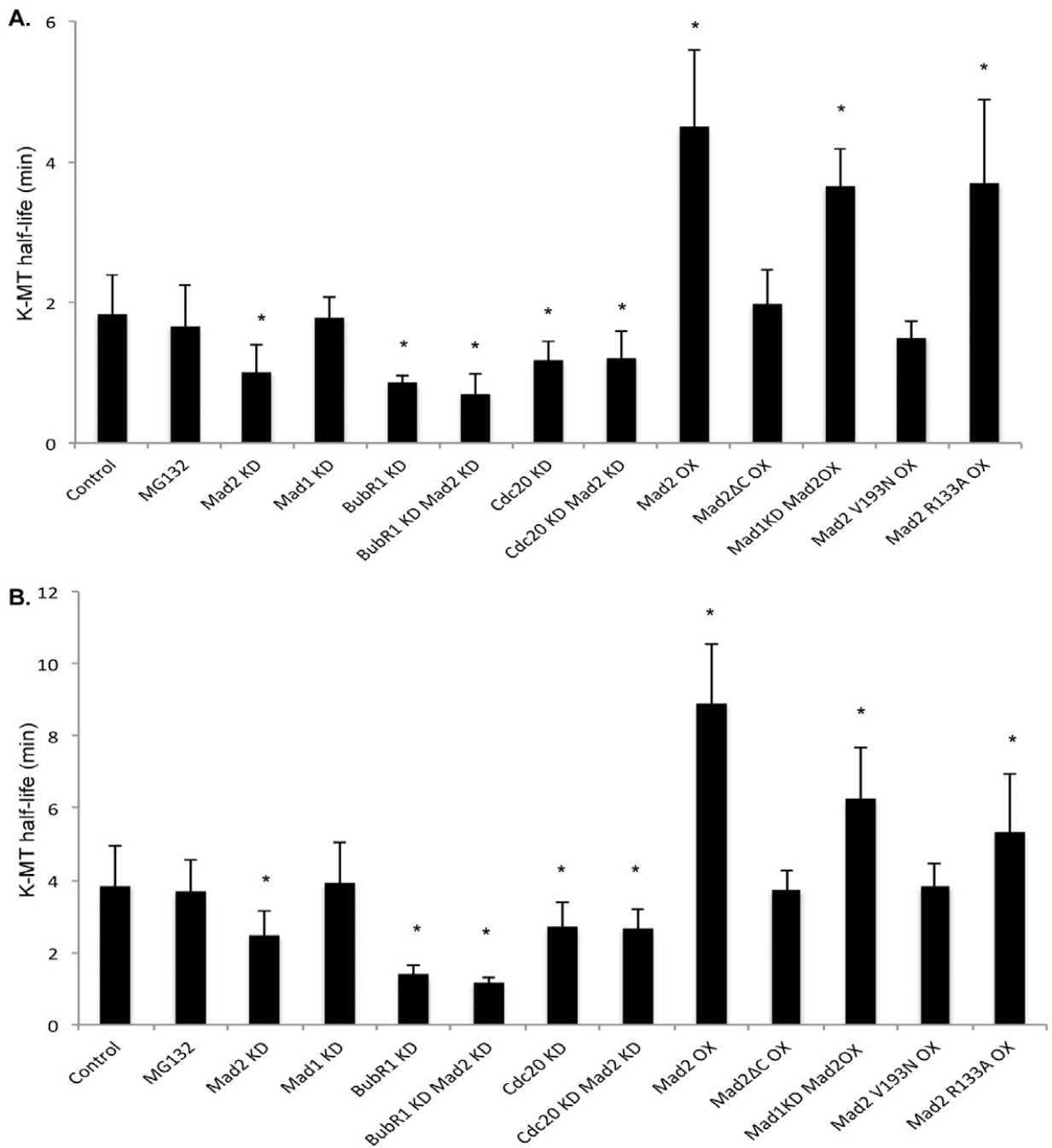


Figure 2. Kinetochores-microtubule half-life. kMT half-life calculated from the exponential decay curve of photoactivated fluorescence ($r^2 > 0.99$) under different conditions for (A) prometaphase and (B) metaphase. Error bars represent SD, * $p < 0.05$, t-test, $n = 10-20$ cells.

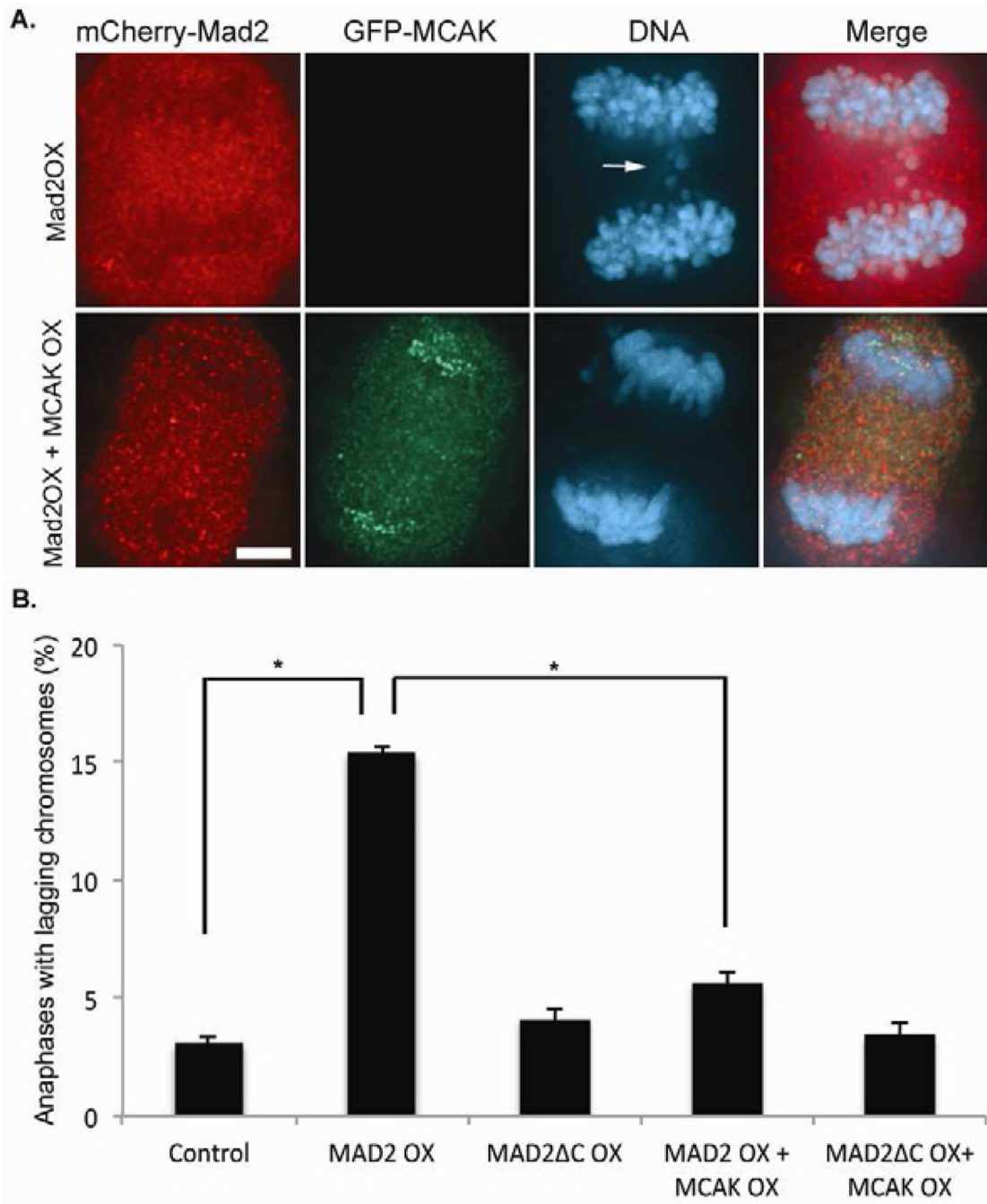
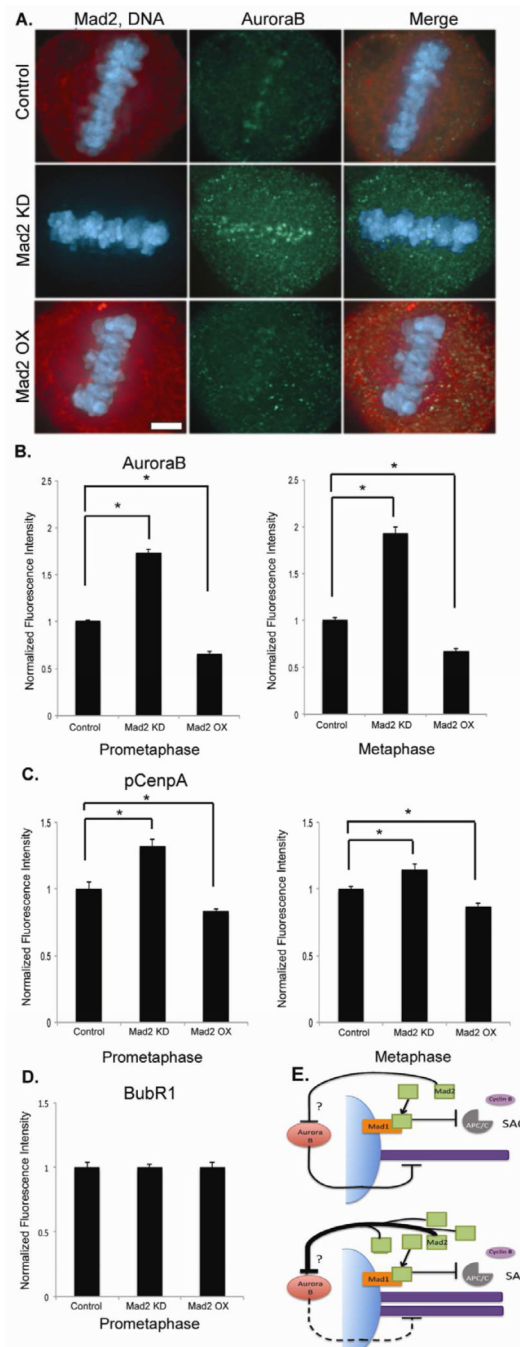


Figure 3.

MCAK overexpression suppresses lagging chromosomes in anaphase in Mad2 overexpressing cells. (A) Anaphase in RPE-1 cells expressing mCherry-Mad2 (red) alone or both mCherry-Mad2 and GFP-MCAK (green) and stained for DNA (blue). The lagging chromosomes induced by Mad2 overexpression are highlighted by an arrow. Scale bar 5 μ m. (B) Number of anaphases with lagging chromosomes in untreated RPE-1 cells (control) and RPE-1 cells overexpressing mCherry-Mad2 (Mad2OX), mCherry-Mad2 Δ C (Mad2 Δ COX), mCherry-Mad2 and GFP-MCAK (Mad2OX + MCAK OX), and mCherry-Mad2 Δ C and GFP-MCAK (Mad2 Δ COX + MCAK OX). Bars represent mean \pm s.e.m., * p <0.05, t-test, n =300 cells of three experiments.

**Figure 4.**

Mad2 affects Aurora B localization and activity at the centromeres. (A) Metaphase of untreated RPE-1 cells (control) and RPE-1 cells overexpressing Mad2 (Mad2OX) and depleted of Mad2 (Mad2KD). Scale bar 5 μ m. Fluorescence intensities of centromeres stained for (B) Aurora B and (C) phosphorylated CenpA (pCenpA) in RPE1 cells normalized using CREST in both prometaphase and metaphase. (D) Fluorescence intensity of BubR1 at kinetochores in prometaphase. Bars represent mean \pm s.e.m., * $p < 0.05$, t-test, $n = 150$ – 200 kinetochore pairs (15–20 cells) of three experiments. (E) Model for Mad2 stabilization of kinetochore-microtubules. Mad2 promotes k-MT stability by attenuating the destabilizing effect of Aurora B activity on k-MT attachments. The question mark refers to

intermediate components of this pathway that lie between Mad2 and Aurora B that are yet to be identified. Overexpression of Mad2 excessively suppresses Aurora B activity resulting in hyperstable k-MT attachments.